Original Article | Gastrointestinal Imaging

http://dx.doi.org/10.3348/kjr.2014.15.3.334
pISSN 1229-6929 · eISSN 2005-8330
Korean J Radiol 2014;15(3):334-345

Korean Journal of Radiology
KJR

CT Findings of Gallbladder Metastases: Emphasis on Differences According to Primary Tumors

Won Seok Choi, MD[1], Se Hyung Kim, MD[1], Eun Sun Lee, MD[1], Kyoung-Bun Lee, MD[2], Won Jae Yoon, MD[3], Cheong-Il Shin, MD[1], Joon Koo Han, MD[1]

Departments of [1]Radiology and [2]Pathology, Seoul National University Hospital, Seoul 110-744, Korea; [3]Department of Internal Medicine, Inje University Seoul Paik Hospital, Inje University College of Medicine, Seoul 100-032, Korea

Objective: To describe computed tomography (CT) features of metastatic gallbladder (GB) tumors (MGTs) from various primary tumors and to determine whether there are differential imaging features of MGTs according to different primary tumors.

Materials and Methods: Twenty-one patients who had pathologically confirmed MGTs and underwent CT were retrospectively enrolled. Clinical findings including presenting symptoms, type of surgery, and interval between primary and metastatic tumors were recorded. Histologic features of primary tumor and MGTs including depth of invasion were also reviewed. Imaging findings were analyzed for the location and morphology of MGTs, pattern and degree of enhancement, depth of invasion, presence of intact overlying mucosa, and concordance between imaging features of primary and metastatic tumors. Significant differences between the histologies of MGTs and imaging features were determined.

Results: The most common primary tumor metastasized to the GB was gastric cancer (n = 8), followed by renal cell carcinoma (n = 4) and hepatocellular carcinoma (n = 3). All MGTs (n = 21) manifested as infiltrative wall thickenings (n = 15) or as polypoid lesions (n = 6) on CT, similar to the features of primary GB cancers. There were significant differences in the morphology of MGTs, enhancement pattern, enhancement degree, and depth of invasion according to the histology of primary tumors ($p < 0.05$). Metastatic adenocarcinomas of the GB manifested as infiltrative and persistently enhancing wall thickenings, while non-adenocarcinomatous metastases usually manifested as polypoid lesions with early wash-in and wash-out.

Conclusion: Although CT findings of MGTs are similar to those of primary GB cancer, they are significantly different between the various histologies of primary tumors.

Index terms: *Gallbladder; Neoplasms; Metastasis; CT; MRI*

Received November 11, 2013; accepted after revision March 15, 2014.
This study was supported by a grant from the Seoul National University Hospital Research Fund No. 03-2013-390.

Corresponding author: Se Hyung Kim, MD, Department of Radiology and the Institute of Radiation Medicine, Seoul National University Hospital, 101 Daehak-ro, Jongno-gu, Seoul 110-744, Korea.
• Tel: (822) 2072-2057 • Fax: (822) 743-6385
• E-mail: shkim7071@gmail.com

This is an Open Access article distributed under the terms of the Creative Commons Attribution Non-Commercial License (http://creativecommons.org/licenses/by-nc/3.0) which permits unrestricted non-commercial use, distribution, and reproduction in any medium, provided the original work is properly cited.

INTRODUCTION

Although metastasis to the gallbladder (GB) is rare and usually manifests at a late and advanced stage of malignancy, it has recently garnered increasing attention by virtue of advances in the fields of medical oncology and surgery. A recent article in which the clinicopathologic characteristics of 20 patients with metastatic GB tumors (MGTs) were analyzed reported a survival benefit of curative cholecystectomy for MGTs even in an advanced stage of malignancy (1). Also, there was a tendency to achieve

Korean Journal of Radiology
KJR

more complete curative (R0) resection in patients with a preoperative diagnosis of MGTs than in patients without a preoperative diagnosis (1). Therefore, when GB lesions are newly detected in known cancer patients, the diagnosis of MGTs may alter management decisions and positively affect prognosis.

Reports have described the imaging findings of MGTs, but most have been case reports (2-7) and the majority of primary tumors were determined to be melanomas (2-4), lung cancers, and renal cell carcinomas (RCCs) (5-7). Furthermore, in an autopsy series, melanoma was shown to account for more than half of all metastatic lesions involving the GB (8). According to a recent publication, however, gastric cancer was the most common primary tumor metastasized to the GB (1). Despite such a discrepancy, there have been few reports systematically analyzing the incidence of MGTs based on routine clinical practice rather than in autopsy series. Furthermore, only a few reports have addressed the imaging features of MGTs from primary tumors other than melanomas or RCCs. Although one report described a spectrum of imaging findings in 13 patients with GB metastasis (9), the focus was on ultrasonography. Due to the many advantages of computed tomography (CT), which include recent advancements in detector technology and three-dimensional software, wide availability, cheap cost, and easy standardization, CT has become an essential first-line imaging modality in oncology. Therefore, radiologists should be familiar with the CT features of MGTs.

Considering that metastasis to the gastrointestinal (GI) tract shows characteristic imaging features of a "target" or "bull's-eye" pattern with an intact overlying mucosal layer at the anti-mesenteric border (10), we hypothesized that MGTs would appear as lesions with intact overlying layer, different from that of primary GB cancer. However, to the best of our knowledge, no reports have described the imaging features of MGTs compared to those of primary GB cancers. Herein, we describe the CT findings of MGTs from various primary malignancies and attempt to determine whether there are characteristic imaging features of MGTs, which may differ from primary GB cancers, and whether there are differential imaging features based on the various histologies of primary tumors.

MATERIALS AND METHODS

The institutional review board of our hospital approved this study and waived requirement for patients' informed consent due to the retrospective nature of this study.

Study Population

We searched the pathology department database for cases of MGTs diagnosed between January 2001 and March 2013. The study population of this study was determined as follows. First, we selected all patients with pathologic reports including the terms "gallbladder metastasis", "metastatic adenocarcinoma and gallbladder", and "metastatic tumor and gallbladder". Sixty-three individuals were chosen in this step. Second, one author reviewed all the detailed pathologic reports and excluded 34 cases with direct tumor invasion to the GB (n = 31) and serosal implants (n = 3). Third, two radiologists reviewed all the CT examinations and excluded eight cases that met the following criteria: 1) no available CT examinations (n = 3) and 2) no demonstrable abnormal finding in the GB (n = 5). Finally, 21 patients (15 men and 6 women) with a mean age of 63.8 years (age range: 28–77 years) were included in this study. Our study population included a subset (n = 13) of patients from a previous clinical study regarding MGTs (1). All primary tumors except three hepatocellular carcinomas (HCCs) were confirmed by histology and all MGTs were histologically confirmed by cholecystectomy. All HCCs were confirmed by a combination of clinical findings (liver cirrhosis), imaging (CT and angiography), and/or laboratory findings (alpha-fetoprotein > 200 ng/mL).

Clinical and Histologic Features

The clinical features of the patients were analyzed by one author using the electronic medical records of our hospital. For the primary malignancy, location, histologic type, and tumor, node, and metastasis (TNM) staging were recorded. For metastatic GB tumors, the following features were analyzed: 1) presentation with acute cholecystitis, 2) laboratory abnormalities including total bilirubin or human serum C-reactive protein (hs-CRP), and 3) interval between primary malignancy and GB metastasis (months). Acute cholecystitis was diagnosed with a combination of clinical (fever, right upper quadrant pain, Murphy's sign), laboratory (elevated bilirubin or hs-CRP level), and/or imaging findings described below. All laboratory findings were recorded from tests performed closest to the CT examinations. Total bilirubin level was available in all patients, but the level of hs-CRP was only available in 11 patients.

For histologic analysis of MGTs, microscopic slides of the patients were re-evaluated by an experienced hepatobiliary

pathologist in terms of depth of invasion by the tumor and the presence of intact overlying epithelium.

CT Acquisition

Patients fasted for at least 6 hours prior to the examination; no oral contrast agent or water was given to the patients. All 21 patients underwent CT examinations using one of seven CT scanners. All CT scans except four were performed with multidetector CT (MDCT) scanners; Mx 8000 4-channel MDCT (Marconi Medical Systems, Cleveland, OH, USA) in six patients, LightSpeed Ultra 8-channel (GE Medical Systems, Milwaukee, WI, USA) in four patients, Mx 8000 IDT 16-channel (Philips Medical Systems, Cleveland, OH, USA) in one patient, Brilliance 64-channel (Philips Medical Systems, Cleveland, OH, USA) in three patients, Discovery 750 HD 64-channel (GE Medical Systems, Milwaukee, WI, USA) in two patients, and Aquilion ONE 320-channel (Toshiba Medical Systems, Otawara, Japan) in one patient. The remaining four CT scans were performed with a single-detector CT scanner (SDCT); Somatom Plus 4 (Siemens Medical Systems, Forchheim, Germany) in three patients and SCT-7800 TE (Shimadzu Corporation, Kyoto, Japan) in one patient. For MDCT examinations, the scanning parameters were detector configuration, 0.625–2.5 mm; pitch, 0.891–1.5; rotation time, 0.5–0.75 seconds; 120 kVp; 150–250 mAs; slice thickness/reconstruction interval, 2.5–5/1.25–5 mm. For single-detector CT, acquisition parameters were slice thickness/reconstruction interval of 3–5/3–5 mm, pitch of 1, rotation time of 1 second, 120 kVp, and 200 mAs. For all patients, 1.5 mL/kg of a 370 mgI/mL iodinated contrast agent was administered at a rate of 3–5 mL/sec. CT images were obtained at a single phase of portal venous phase (n = 4), double phases including the precontrast and portal venous phase (n = 2) or including arterial and portal venous phases (n = 2), triple phases including the precontrast, arterial, and portal venous phase (n = 12), or quadruple phases including the precontrast, arterial, portal venous, and delayed phase (n = 1). For arterial phase, a delay time of 13–17 seconds was used after the attenuation of the descending aorta reached 100 Hounsfield units using the bolus tracking technique. Portal venous and delay phase scanning were performed 60–75 seconds and 3 minutes after contrast agent administration, respectively. In 10 (47.6%) of 21 patients, coronal and sagittal multiplanar reconstruction (MPR) images were reconstructed.

Image Analysis

Two radiologists reviewed all CT images without knowledge of the primary tumor or extent of disease on histology. All decisions on imaging findings were made by consensus. All CT features of MGTs were evaluated on a picture archiving and communications system as follows: 1) location of the lesion, 2) morphology, 3) degree and pattern of enhancement of the lesion on CT, 4) presence of intact overlying mucosal layer, 5) depth of the invasion on CT, 6) presence of accompanying cholecystitis, 7) concordance of imaging findings between the primary malignancy and MGTs, and 8) synchronicity of the primary malignancy and MGTs. Location of MGTs was subdivided into the cystic duct, neck, body, and fundus. If the lesion was located at more than two sites, it was described as diffuse or multifocal involvement according to morphology. Morphology of the lesions was subcategorized into infiltrative, mass-forming, and polypoid types. The lesion was considered as infiltrative when it appeared as a diffuse or focal wall thickening of the GB. The lesion was regarded as polypoid when it appeared as a nodule protruding into the lumen. Mass-forming referred to the replacement of the GB by the mass. The degree of enhancement of the lesion was reported as low, iso, or high attenuation as compared to that of adjacent normal GB mucosa on each phase. In the cases accompanied by acute cholecystitis on CT, the degree of enhancement of the lesion was compared with that of normal extrahepatic bile duct. The pattern of enhancement was characterized as persistent enhancement, early wash-in and wash-out, or a persistent low pattern. The lesion was classified as showing persistent enhancement when attenuation on arterial/portal phases was low/high, iso/high, or high/high compared to the adjacent normal GB or bile duct mucosa; as an early wash-in and wash-out pattern when the lesion showed high/low or high/iso attenuation; and as a persistent low pattern for lesions with low/low attenuation. The depth of invasion of the lesion was determined using previously defined CT staging criteria of primary GB cancer as described below (11, 12). However, to avoid confusion between T staging for primary GB cancer and depth of invasion for MGTs, we used a modified term "mT staging" for MGTs. In 11 cases with available coronal or sagittal MPR images, MPR images as well as axial images were also reviewed.

The criteria of CT findings for each mT stage were mT1 (to muscle layer), polypoid lesions without focal thickening of the GB wall or focal nodular or flat thickening of the inner

Korean Journal of Radiology
KJR

enhancing layer of the GB wall with clear, low-attenuated outer wall; mT2 (to perimuscular connective tissue [PMCT] layer), diffuse wall thickening with obliteration of the layered pattern, diffuse wall thickening with strong, thick inner wall enhancement and weak enhancement of the outer layer (two-layered pattern), or focal wall thickening with outer surface dimpling at the tumor base; mT3, enhancing GB wall thickening with prominent pericholecystic infiltration or direct invasion to the liver or one other adjacent organ; and mT4, tumor invades main portal vein or hepatic artery or invades more than two extrahepatic organs or structures. For mT2 lesions, there should be the presence of an apparently smooth fat plane separating between the lesion and the adjacent organs. Because even MDCT cannot differentiate mucosal layer from the muscle layer of the GB, we did not try to distinguish between mT1a (confined to mucosa) and mT1b (invades to the muscle) on CT. For the presence of an intact mucosal layer, radiologists deemed it intact when the innermost layer was not disrupted nor enhanced by the tumor. For the presence of accompanying cholecystitis, well-known imaging features of acute cholecystitis were used: distended and diffusely thickened GB wall with or without pericholecystic infiltration, fluid collection, or hyperemia at GB bed of the liver. If the enhancement pattern and degree were similar between the primary tumor and GB metastasis, radiologists recorded it as concordant; if not, it was recorded as discordant. In terms of the presence of intact overlying mucosa and the depth of invasion, CT findings were correlated with histologic findings and the concordance between imaging and histologic findings were also recorded.

Statistical Analyses

To determine significant differences between the histology of MGTs and CT features, chi-square or Fisher's exact tests were used. Two-sided p values < 0.05 were considered to indicate statistical significance. All analyses were performed using SPSS for Windows version 19.0 (SPSS Inc., Chicago, IL, USA).

RESULTS

Clinical and Histopathologic Features

Eight patients (38.1%) presented with clinical features of acute cholecystitis. Total bilirubin level was abnormally elevated in two patients (9.5%) and hs-CRP level was abnormally elevated in all 11 patients in whom hs-CRP level were checked. Mean value of hs-CRP level was 13.31 ± 9.81 mg/dL (range, 1.97–31.55 mg/dL). GB metastasis was diagnosed synchronously with primary malignancy in seven (33.3%) and metachronously in 14 (66.7%) patients. The mean interval between the diagnosis of primary malignancy and GB metastasis in the latter 14 patients was 46.3 months (range, 3.4–197.2 months).

The most common primary tumor metastasized to the GB was gastric cancer (n = 8, 38.1%), followed by RCC (n = 4, 19.0%), HCC (n = 3, 14.3%), and colorectal cancer (n = 2, 9.5%). In one case each, ovarian cancer, duodenal cancer, malignant melanoma, and uterine cervix cancer also metastasized to the GB. Primary tumors in the GI tract (n = 11) and ovary (n = 1) were all adenocarcinomas, of which five were moderately-differentiated adenocarcinomas and four were poorly-differentiated adenocarcinoma. The remaining three adenocarcinomas were mucinous, signet ring cell carcinomas, and an ovarian serous cystadenocarcinoma. In two patients with RCC and uterine cervix cancer, information regarding T and N staging of primary tumors was not available. For the remaining patients, T and N staging of primary tumors was variable from T1N0 to T4bN3 (Table 1). In eight patients (38.1%), distant metastasis (M1) including MGTs was detected at the initial diagnosis of the primary tumor.

Microscopic slides for MGTs were available in 17 patients (81.0%) and were re-evaluated. Histologic findings are summarized in Table 1. On retrospective review of histopathology, metastatic tumors invaded from the serosa to the mucosa in five patients, from serosa to PMCT in one, from PMCT to the mucosa in two patients, confined to PMCT in four, and confined to the mucosa in five. In 13 (76.5%) of 17 MGTs, the innermost lining epithelium of the GB was intact while it was eroded and denuded in the remaining four (23.5%) tumors on microscopy. Although metastatic tumors invaded the mucosa in 12 patients, tumor cells were mainly located at the subepithelial layer (lamina propria). This differed from primary GB cancers in which the epithelium is the origin of the tumors and replaced by the tumors.

CT Findings

Computed tomography findings are summarized in Table 1 and representative examples are presented in Figures 1–4. Metastasis of primary malignancy to the GB was located at the cystic duct in three patients (14.3%), at the neck of the GB in five (23.8%), the body of the GB in

Table 1. CT and Histologic Findings in 21 Patients with Gallbladder Metastasis from Various Primary Tumors

No.	Primary Site/ Staging	Location	Morphology	Enhancement Degree		Enhancement Pattern	Overlying Layer		Depth of Invasion (Organ of Invasion)		Cholecystitis	
				AP	PP		CT	Histology	CT*	Histology	CT	Clinical
1	Stomach/T4aN3M0	Diffuse	Infiltrative	N/A	High	N/A	-	+	mT4 (duodenum, colon)	Serosa to mucosa‡	-	+
2	Stomach/T4aN0M0	Body	Infiltrative	N/A	Low	N/A	+	+	mT3 (colon)	Serosa to PMCT	-	-
3	Stomach/T4aN2M0	Neck	Infiltrative	High	High	Persistent enhancement	-	+	mT2	Serosa to mucosa‡	+	+
4	Stomach/cT4bN3M1	Diffuse	Infiltrative	High	High	Persistent enhancement	-	N/A	mT3 (serosa)	N/A	-	-
5	Stomach/T4aN3M0	Cystic duct	Infiltrative	N/A	High	N/A	-	+	mT2	PMCT only	+	+
6	Stomach/T4aN3M0	Body	Infiltrative	High	High	Persistent enhancement	-	+	mT2	PMCT to mucosa‡	+	+
7	Stomach/T3N3M0	Cystic duct	Infiltrative	High	High	Persistent enhancement	-	+	mT2	PMCT to mucosa‡	+	+
8	Stomach/cT4aN3M1	Cystic duct	Infiltrative	High	High	Persistent enhancement	-	+	mT2	PMCT only	+	+
9	Kidney/TxNxM0†	Neck	Polypoid	High	High	Early wash-in/wash-out	-	N/A	mT1	N/A	-	-
10	Kidney/T2bN0M1	Neck	Polypoid	N/A	High	N/A	-	+	mT1	Mucosa only‡	+	+
11	Kidney/T3bN0M0	Neck	Polypoid	High	Iso	Early wash-in/wash-out	-	-	mT1	Mucosa only	+	+
12	Kidney/T1N0M0	Body	Polypoid	High	Iso	Early wash-in/wash-out	-	+	mT1	Mucosa only‡	-	-
13	Liver/cT2N0M0	Body	Polypoid	High	Iso	Early wash-in/wash-out	-	-	mT1	Mucosa only	-	-
14	Liver/cT3bN0M1	Body	Infiltrative	High	Iso	Early wash-in/wash-out	-	+	mT2	PMCT only	-	-
15	Liver/cT3bN0M1	Body	Infiltrative	High	Iso	Early wash-in/wash-out	-	+	mT3 (serosa)	PMCT only	-	-
16	Colon/T3N1bM1	Neck	Infiltrative	Low	Low	Persistent low	-	N/A	mT3 (serosa)	N/A	-	-
17	Colon/T4bN1M1	Fundus	Infiltrative	N/A	High	N/A	-	N/A	mT2	N/A	-	-
18	Ovary/T3cN1M0	Fundus	Infiltrative	High	High	Persistent enhancement	-	-	mT3 (liver bed)	Serosa to mucosa	-	-
19	Skin/T3aN0M0	Body	Polypoid	High	High	Persistent enhancement	-	+	mT1	Mucosa only‡	-	-
20	Duodenum/T4N0M1	Diffuse	Infiltrative	High	High	Persistent enhancement	-	-	mT3 (serosa)	Serosa to mucosa	-	-
21	Cervix/TxNxM0†	Body	Infiltrative	N/A	Low	N/A	+	+	mT3 (liver bed)	Serosa to mucosa‡	-	-

Note.— *On CT, depth of invasion for T staging (mT) of metastatic tumors was determined from mucosa based on staging system of primary gallbladder cancer, †Information regarding TN staging was not available, ‡Metastatic tumor invaded to subepithelial layer (lamina propria), preserving epithelial lining. AP = arterial phase, N/A = not available, PMCT = perimuscular connective tissue, PP = portal phase

Korean Journal of Radiology
KJR

A B

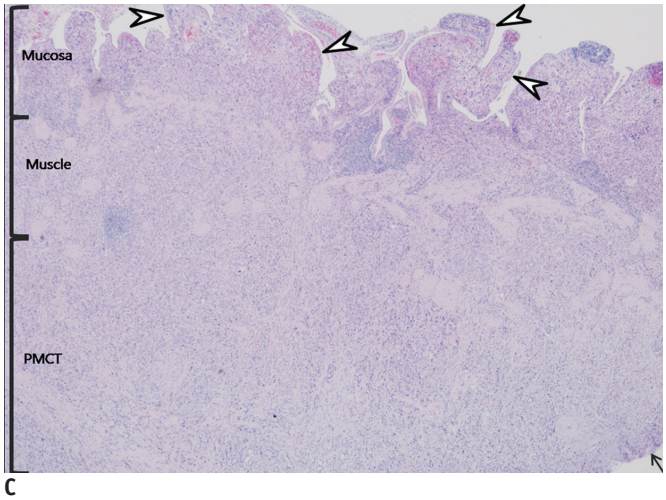

C

Fig. 1. Infiltrative type metastatic gallbladder (GB) cancer from gastric adenocarcinoma in 62-year-old man presenting with acute right upper quadrant pain (case 3). Patient had undergone subtotal gastrectomy for stomach cancer 4 years ago. Pathologic tumor, node, and metastasis staging of gastric cancer was T4aN2.

A. Arterial (left) and portal (right) phase CT images show focal, full-thickness, enhancing wall thickening (arrows) with obliteration of layered pattern at neck of GB. There was no intact overlying mucosa. Lesion is manifested as infiltrative type of GB cancer with persistent enhancement. Outer margin of thickened wall seemed to be clear, therefore, depth of invasion on CT was regarded as mT2 (invasion to perimuscular connective tissue). Edematous wall thickening is noted at GB (*) and surrounding transient hepatic attenuation difference (arrowheads) is observed at GB bed of liver, suggesting accompanying acute cholecystitis. **B.** Coronal CT images on portal phase clearly show enhancing wall thickening (arrows) at neck of GB. Marked luminal distention and edematous wall thickening of GB (*) suggest acute cholecystitis. **C.** Photomicrograph (hematoxylin and eosin, x 40) obtained after open cholecystectomy reveals metastatic adenocarcinoma invades from serosa (arrow) to mucosa. Therefore, depth of tumor invasion was regarded as mT3 based on staging system of primary GB cancer. Although tumor cells invade into mucosal layer, they are mainly located at lamina propria (subepithelial layer) and overlying surface epithelium (arrowheads) is intact. PMCT = perimuscular connective tissue

eight (38.1%), and fundus of the GB in two (9.5%). In the remaining three patients (14.3%), the metastatic tumor involved the GB diffusely. In terms of the morphology, infiltrative type was found in 15 patients (71.4%) (Figs. 1, 2) and polypoid type in six (28.6%) (Figs. 3, 4). In six patients, the degree of enhancement on arterial phase and the enhancement pattern could not be evaluated due to the absence of arterial phase images. For the enhancement pattern of 15 patients who had both arterial and portal phase images, eight patients (53.3%) showed persistent enhancement (Figs. 1, 2), six (40%) demonstrated early wash-in and wash-out (high attenuation on arterial phase and low/iso attenuation on portal phase) (Figs. 3, 4), and one patient (6.7%) showed persistent low enhancement (low attenuation on both arterial and portal phases). Of these 15 cases, 14 MGTs showed higher enhancement than the adjacent normal GB or bile duct mucosa while one lesion showed lower attenuation on arterial phase images. On portal venous phase, the degree of enhancement of the lesions was higher than the adjacent normal mucosa in 13

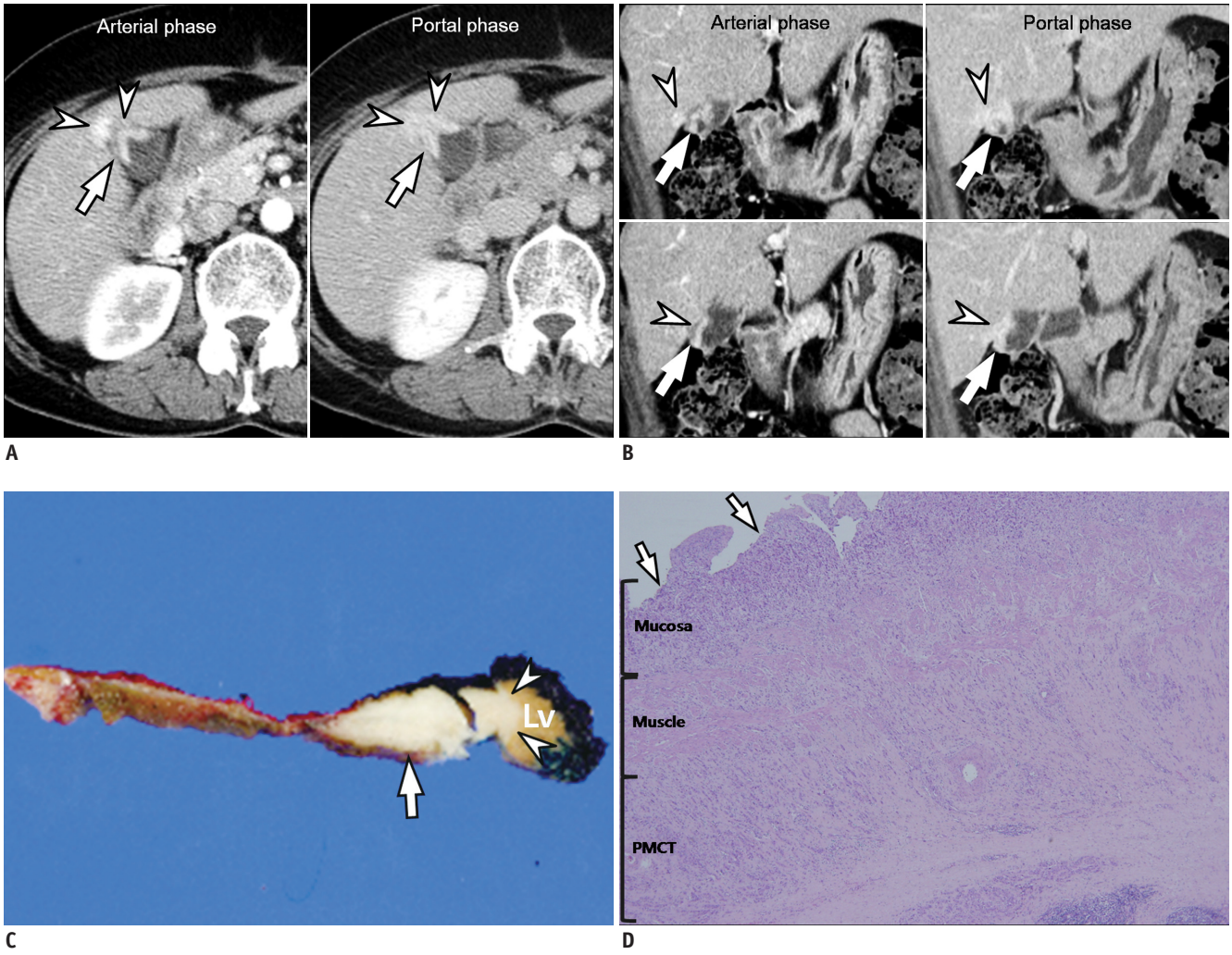

Fig. 2. Infiltrative type metastatic gallbladder (GB) cancer from ovarian serous adenocarcinoma in 60-year-old woman. In this patient, GB wall thickening was detected during surveillance after left salphingo-oophorectomy for ovarian cancer (case 18).
A, B. Axial **(A)** and coronal **(B)** CT images show focal and full-thickness wall thickening (arrows) at fundus of GB. Lesion shows strong enhancement on arterial phase (left) and persistent enhancement on portal phase (right). Tumor seems to invade into adjacent liver parenchyma (arrowheads); therefore, depth of tumor invasion was regarded as mT3 (invasion to serosa or one adjacent organ) on CT. Overlying innermost layer is not preserved. **C.** On photograph of cut surface of gross specimen obtained after extended cholecystectomy, there is focal wall thickening (arrow) at fundus of GB, which directly invades into liver (Lv) bed (arrowheads). Depth of tumor was regarded as mT3. **D.** On low-power (hematoxylin and eosin, x 40) photomicrograph, metastatic tumor cells invade full thickness of GB wall from mucosa to perimuscular connective tissue (PMCT) and serosa (not shown). Adjacent liver bed is also invaded by tumor cells (not shown). Overlying epithelium is denuded (arrows).

(61.9%), similar in five (23.8%), and lower in three cases (14.3%). On CT, six (28.6%) MGTs were staged as mT1 and they were all of polypoid type (Figs. 3, 4). Seven lesions (33.3%) were staged as mT2 (invaded to PMCT) (Fig. 1), seven (33.3%) as mT3 (serosa or one organ invasion) (Fig. 2), and one (4.8%) as mT4 (invasion to two or more organs). Of seven mT3 lesions, four lesions were regarded as invading the serosal layer and the remaining three lesions seemed to invade into one adjacent organ (two to the liver bed and one to the colon) (Fig. 2). One mT4 lesion seemed to invade the adjacent duodenum and colon. CT showed an intact mucosal layer in only two patients (9.5%). Except in these two patients showing intact overlying mucosa, imaging findings of MGTs were not different from those of primary GB cancers. Seven patients (33.3%) showed CT evidence of acute cholecystitis (Fig. 1), while 14 (66.7%) did not. Correlating with clinical findings in terms of acute cholecystitis, 20 patients (95.2%) showed the same results (7 with cholecystitis and 13 without cholecystitis) on both imaging and clinical findings. The remaining one patient (4.8%) showed discrepant results between CT and clinical findings in terms of accompanying cholecystitis: the patient had clinical findings of cholecystitis (right upper quadrant pain, fever, and elevated hs-CRP to 6.9 mg/dL)

Korean Journal of Radiology
KJR

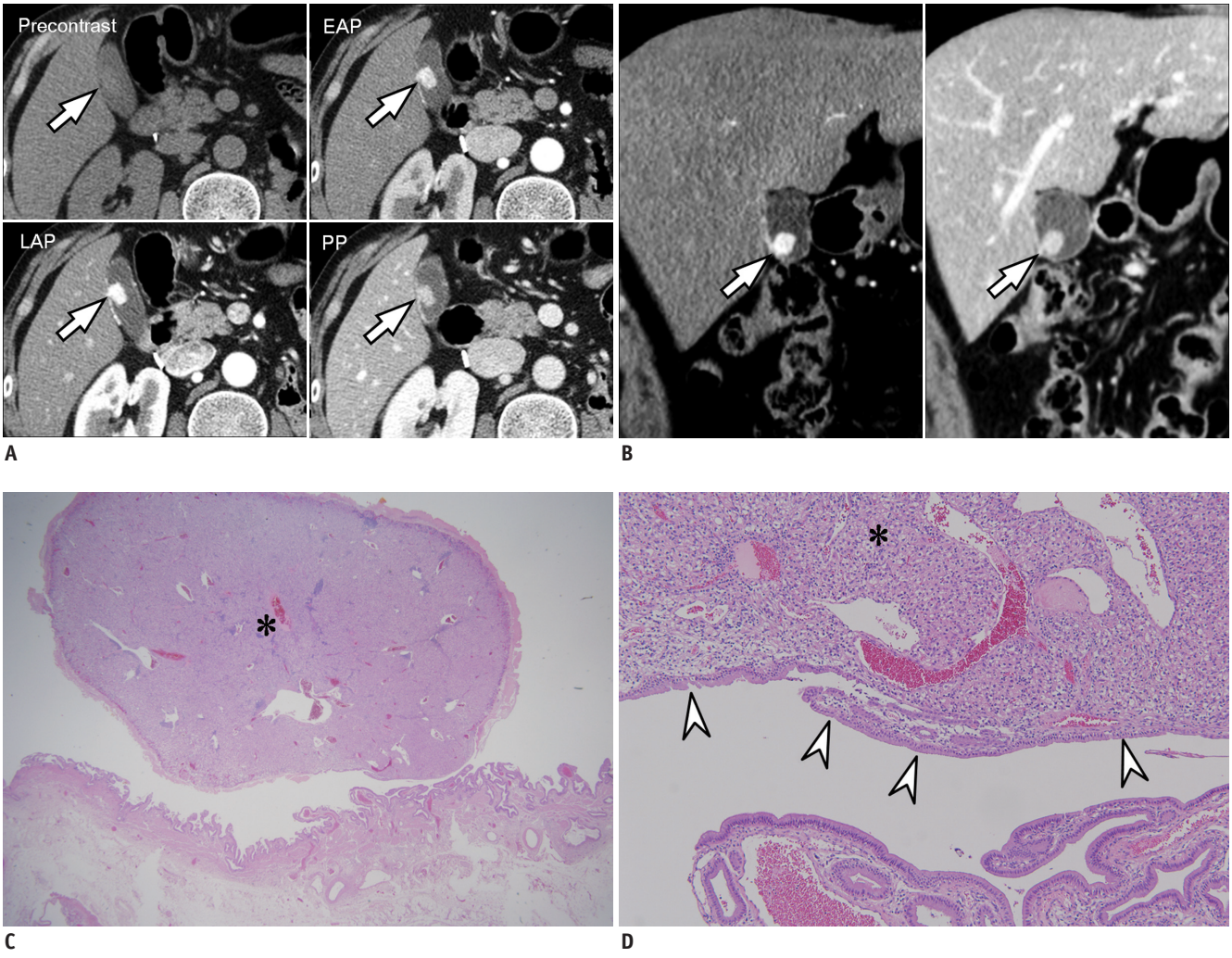

Fig. 3. Polypoid type metastatic gallbladder (GB) cancer from renal cell carcinoma (RCC) in 50-year-old man. In this patient, polypoid GB lesion was incidentally found during surveillance after left nephrectomy for RCC 11 years ago (case 12). Pathologic tumor, node, and metastasis staging of RCC was T1bN0.
A, B. Axial **(A)** and coronal **(B)** CT images show 1.3 cm polypoid lesion (arrows) in body of GB. Lesion shows strong enhancement (early wash-in) on early (EAP) and late arterial phase (LAP) images and wash-out on portal phase (PP) image. GB wall adjacent to lesion does not seem to be thickened; therefore, CT stage was regarded as mT1. Laparoscopic cholecystectomy demonstrates 1.3 cm polypoid lesion in GB (not shown). **C.** Photomicrograph (hematoxylin and eosin [H&E], x 12.5) shows polypoid tumor (*) containing renal cell carcinoma cells. **D.** Magnified photomicrograph (H&E, x 100) demonstrates that tumor cells (*) are confined to subepithelial layer (lamina propria) and overlying surface epitheliums (arrowheads) are intact. On microscopy, depth of tumor was regarded as mT1.

without CT evidence of acute cholecystitis. The concordance of imaging findings such as enhancement pattern and/or morphology between primary and metastatic lesions was able to be evaluated in 16 of 21 patients (76.2%). Of those 16 cases, 13 (81.3%) revealed concordant imaging findings between primary and metastatic lesions, while three (18.7%) revealed discordant imaging findings.

Comparison between CT and Histologic Findings

Comparison between CT and histologic results is summarized in Table 1. In terms of the intact overlying mucosa, imaging and histologic results were concordant in six (35.3%) of the 17 patients whose microscopic slides were available and discordant in 11 (64.7%). In two of six patients showing concordant results regarding intact innermost layer, the innermost epithelial layer was preserved on both imaging and histology. In all 11 patients showing discordant results, the innermost epithelial layer was preserved on histology but appeared to be invaded by the tumor on CT.

Regarding the depth of tumor invasion, CT and histologic results were concordant in 15 (88.2%) of 17 patients (Figs. 2-4) and discordant in two (11.8%) (Fig. 1). All except one mT2- and one mT3-equivalent MGTs were correctly

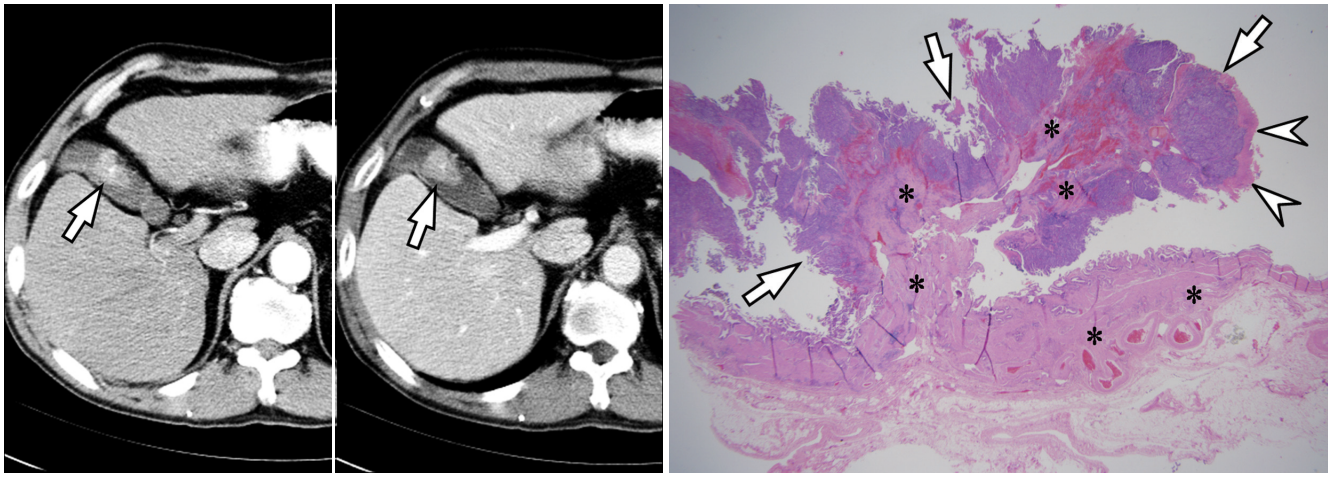

A B

Fig. 4. Polypoid type metastatic gallbladder (GB) cancer from hepatocellular carcinoma (HCC) in 75-year-old man. Polypoid GB lesion was incidentally found during surveillance after transarterial chemoembolization for HCC nodules at segment IV of liver 2 years ago (case 13).

A. On dynamic CT image, 2.6 cm polypoid lesion (arrows) is demonstrated at body of GB. Lesion seems to be confined to mucosa and regarded as mT1. Lesion shows early enhancement on arterial (left) phase and wash-out on portal (right) phase images. **B.** Photomicrograph (hematoxylin and eosin, x 12.5) after open cholecystectomy shows that polypoid metastatic HCC (arrows) is confined to mucosal layer and regarded as mT1. Note hemorrhage and inflammatory cell infiltration in muscle layer (*). Overlying surface epithelium was denuded by erosion and covered with fibrin coat (arrowheads).

staged on CT. The two incorrectly staged MGTs were all of infiltrative type. For these two cases, CT underestimated the extent of the tumor (mT3 as mT2) in one and overestimated in another (mT2 as mT3).

Results of Statistical Analysis

The results of statistical analysis between CT findings and histology of MGTs are presented in Table 2. According to the histology of tumors, there were significant differences in the morphology of MGTs (p = 0.001), enhancement pattern (p = 0.019), and enhancement degree on portal phase (p = 0.005). Depth of invasion by metastatic tumors on CT was not statistically different among the various histologies (p = 0.074). However, depth of invasion on CT was significantly between adenocarcinoma and non-adenocarcinomatous tumors (p = 0.009).

All 12 metastatic adenocarcinomas of the GB were of infiltrative type (12/12, 100%) (Figs. 1, 2) while other histologies such as RCC, HCC, melanoma, or squamous cell carcinoma of MGTs tended to be of polypoid type (6/9, 66.7%) (Figs. 3, 4). The difference in tumor morphology between adenomatous and non-adenomatous MGTs was significant (p = 0.002). With regard to the enhancement pattern, metastatic adenocarcinomas usually showed persistent enhancement (7/8, 87.5%) (Figs. 1, 2) while other histologies tended to demonstrate the early wash-in/wash-out pattern of enhancement (6/7, 85.7%) (Figs. 3, 4). This difference in enhancement pattern was also statistically significant (p = 0.003). Adenocarcinomas usually showed higher enhancement (10/12, 83.3%) than adjacent mucosa on portal phase (Figs. 1, 2) while MGTs of other histologies showed similar enhancement or were lower than the adjacent mucosa (6/9, 66.7%) (p = 0.012) (Figs. 3, 4). All metastatic adenocarcinomas of the GB tended to show more than mT2 stage (6 as mT2, 5 as mT3, and 1 as mT4 stage) on CT (Figs. 1, 2) while two-thirds of non-adenocarcinomatous histology were staged as mT1 (6/9, 66.7%) (p = 0.009) (Figs. 3, 4). The degree of enhancement on arterial phase, the presence of intact mucosa and cholecystitis, and concordance between primary and metastatic tumors were not statistically different among the various histologies of MGTs (p = 0.117–0.785).

DISCUSSION

Presently, CT findings of MGTs were significantly different among the various histologies of primary tumors. More specifically, adenocarcinomas metastasized to the GB manifested as infiltrative wall thickenings with persistent enhancement while metastatic RCCs, HCCs, or melanomas of the GB appeared as polypoid lesions with early wash-in or wash-out enhancement. The results were not surprising,

Korean Journal of Radiology
KJR

Table 2. Significant Results of Statistical Analysis between Histology of Metastatic Gallbladder Tumor and Imaging Findings

Histology	CT Findings										
	Morphology		Enhancement Pattern			Enhancement Degree on PP			Depth of Invasion*		
	Infiltrative	Polypoid	Persistent High	Wash-In/Out	Persistent Low	High	Iso	Low	mT1	mT2	mT3	mT4
Adenocarcinoma (n = 12)	12	0	7	0	1	10	0	2	0	6	5	1
RCC (n = 4)	0	4	0	3	0	2	2	0	4	0	0	0
HCC (n = 3)	2	1	0	3	0	0	3	0	1	1	1	0
Melanoma (n = 1)	0	1	1	0	0	1	0	0	1	0	0	0
SCC (n = 1)	1	0				0	0	1	0	0	1	0
P	0.001			0.019			0.005			0.074		
Adenocarcinoma (n = 12)	12	0	7	0	1	10	0	2	0	6	5	1
Non-adenocarcinoma (n = 9)	3	6	1	6	0	3	5	1	6	1	2	0
P	0.002†			0.003			0.012			0.009		

Note.— *On CT, depth of invasion for T staging of metastatic tumors was determined from mucosa based on staging system of primary gallbladder cancer and was described as "mT" staging, †*P* value was calculated using Fisher's exact test. HCC = hepatocellular carcinoma, PP = portal phase, RCC = renal cell carcinoma, SCC = squamous cell carcinoma

given that metastatic tumors typically show similar morphologic and enhancement features as those of primary tumors. Adenocarcinomas of the GI tract usually appear as wall thickenings with delayed enhancement due to abundant desmoplastic tissue within the tumors (13-15). RCCs, HCCs, and melanomas are hypervascular tumors, which show early, strong arterial enhancement and portal washout on CT or MRI (16-18). These results may be helpful for clinicians and radiologists in making a presumptive diagnosis of MGTs in patients with primary tumors and GB lesions simultaneously or metachronously. For instance, if patients with alleged RCC, HCC, or melanoma have a well-enhanced polypoid lesion in the GB, the possibility of MGTs should first be considered, rather than that of GB polyp or polypoid cancer, facilitating a curative resection. Given that curative cholecystectomy for MGTs can provide a survival benefit even in an advanced stage of malignancy and that there is a tendency to achieve more complete curative (R0) resection in patients with a preoperative diagnosis of MGTs than in patients without a preoperative diagnosis (1), a presumptive diagnosis of potentially curative MGTs may have a positive impact on the patients' prognosis.

We also observed that CT features of metastatic GB cancers were indistinguishable from those of primary GB cancers. All MGTs manifested as infiltrative wall thickenings (n = 15) or as polypoid lesions (n = 6), which are two of the three morphologic features of primary GB cancer, namely infiltrative, polypoid, and mass-forming (19-21). We had initially hypothesized that an intact overlying mucosa or epithelium would be frequently found on CT in patients with MGTs, whereas patients with primary GB tumors would not have an intact mucosal layer and, therefore, would be an important differential clue for MGTs from primary GB cancers. Our assumption was based on the fact that tumor implants through hematogeneous spread from the primary tumor may lodge in the subepithelial or muscle layer, sparing the overlying surface epithelium. Indeed, blood-borne metastasis to the GI tract classically appears as multiple subepithelial nodules that often have intact overlying mucosa or may ulcerate to produce the well-known "target" or "bull's-eye" lesions seen on imaging studies (10). However, in contrast to our expectations, CT showed an intact overlying layer of the GB in only two patients with MGTs (2/21, 9.5%). A retrospective histopathologic review of the 17 cases gave us a possible explanation for this discrepancy. Indeed, the overlying epithelium was preserved in 12 out of 17 patients on microscopy. But, as the

metastatic tumor cells spread to the subepithelial, lamina propria layer immediately below the intact, single cell-lined epithelium, due to the limited resolution of CT, even MDCT in separating the histologic layers between the epithelium and lamina propria layer, CT imaging could not differentiate subepithelial tumor spread from intact epithelium. In fact, we observed that CT or MDCT was poor in separating even the mucosal layer from the muscular layer as these two layers were enhanced as one unit or as one complex in the GB due to the absence of submucosa and muscularis mucosa layers (22, 23). Several studies have already reported this difficulty in distinguishing T1 GB cancers into T1a (mucosa invasion) and T1b (proper muscle invasion) cancers on CT or MRI due to their limited resolution (11, 12, 24, 25). With the results of microscopy, we still maintain that this may be a method of differentiating MGTs from primary GB cancers when imaging technology improves sufficiently to distinguish between these layers.

Contrary to the rather big discrepancy regarding the intact overlying layer between CT and histology, a concordant rate for the depth of tumor invasion between CT and histology was high (88.2%). Our result coincides well with that of a previous MDCT study in which the overall accuracy of MDCT for T staging of GB cancer was reported as 83.9% (12). In addition, the percentage of over- and under-staging of tumor invasion on imaging was similar between our (5.9% and 5.9%, respectively) and previous (9.3% and 6.8%, respectively) studies (12). Although the T staging system of primary GB cancer could not directly be applicable to the evaluation for depth of tumor invasion of MGTs, our study results show that CT can potentially evaluate the depth of tumor infiltration even for the metastatic tumors of the GB, helping clinicians or surgeons determine the type or extent of the operation.

Our study results demonstrate that various GI tract tumors, such as gastric, duodenal, or colorectal cancers, can metastasize to the GB. Most publications regarding MGTs from western countries have reported that malignant melanomas, RCCs, breast cancers, and lung cancers are the most common cancers that metastasize to the GB in that order (2-8). In our study, however, gastric cancer was the most common primary tumor metastasizing to the GB, followed by RCC, HCC, and colorectal cancer. This result does not reflect that melanoma is not a common primary site, but rather that the GB may be susceptible to metastasis from various primary tumors. Such a discrepancy in incidence may have primarily resulted from the different geographic epidemiology of cancers. Considering that stomach cancer and HCC are the second and third most common cancers in Eastern countries, respectively, a higher prevalence of MGTs from those tumors may well reflect the high incidence of these primary tumors (1). Accordingly, if infiltrative and persistently enhancing wall thickening in the GB is demonstrated in patients with GI tract cancers, clinicians or radiologists can first consider the possibility of MGTs, especially in Eastern populations. Further studies with a larger study population in different geometric locations are warranted to confirm this observation.

Our study has several limitations. First, it is limited by our relatively small study population, which was unavoidable due to the rarity of MGTs. In addition, there was a potential selection bias toward those with less advanced disease as we recruited all patients with surgically confirmed MGTs. Given that most of the MGTs (particularly adenocarcinomatous MGTs) would not be resectable and were not included in our study population, our results may not be directly applicable to a daily practice of image interpretation, especially for the proportion between adenocarcinomatous and non-adenocarcinomatous MGTs. Nevertheless, we believe that our results are noteworthy because our study is the largest series extensively addressing the clinicopathologic and CT findings of MGTs in a single institution. Second, a higher prevalence of MGTs from gastric cancer and HCC which is different from that of a Western population may be reflected by the high incidence of these primary tumors in our country. Therefore, further study should be conducted with a large and different study population. Third, due to the retrospective nature of this study, it was not possible to use standardized CT protocols. In our study, most patients underwent MDCT, however, four underwent SDCT. Finally, detailed histopathologic results of MGTs were not available in four patients. Therefore, direct comparison between CT and histology regarding the depth of invasion and the presence of intact overlying mucosa could not be performed in those patients.

In conclusion, CT appearances of MGTs are either of infiltrative type or polypoid type and are not distinguishable from those of primary GB cancers. However, imaging findings of MGTs are observed to be significantly different among the various histologies of primary tumors. Metastatic adenocarcinomas usually show infiltrative wall thickenings with persistent enhancement while MGTs from RCC, HCC, or melanoma manifest as well-enhancing polypoid lesions with early wash-out on CT.

Korean Journal of Radiology
KJR

Acknowledgments

We acknowledge Byung Ihn Choi for his advice throughout the preparation of the manuscript and during manuscript revision. We would also like to thank Chris Woo for his English editorial assistance.

REFERENCES

1. Yoon WJ, Yoon YB, Kim YJ, Ryu JK, Kim YT. Metastasis to the gallbladder: a single-center experience of 20 cases in South Korea. *World J Gastroenterol* 2009;15:4806-4809
2. Rehani B, Strohmeyer P, Jacobs M, Mantil J. Gallbladder metastasis from malignant melanoma: diagnosis with FDG PET/CT. *Clin Nucl Med* 2006;31:812-813
3. Guida M, Cramarossa A, Gentile A, Benvestito S, De Fazio M, Sanbiasi D, et al. Metastatic malignant melanoma of the gallbladder: a case report and review of the literature. *Melanoma Res* 2002;12:619-625
4. Vernadakis S, Rallis G, Danias N, Serafimidis C, Christodoulou E, Troullinakis M, et al. Metastatic melanoma of the gallbladder: an unusual clinical presentation of acute cholecystitis. *World J Gastroenterol* 2009;15:3434-3436
5. Ghaouti M, Znati K, Jahid A, Zouaidia F, Bernoussi Z, El Fakir Y, et al. A gallbladder tumor revealing metastatic clear cell renal carcinoma: report of case and review of literature. *Diagn Pathol* 2013;8:4
6. Chung PH, Srinivasan R, Linehan WM, Pinto PA, Bratslavsky G. Renal cell carcinoma with metastases to the gallbladder: four cases from the National Cancer Institute (NCI) and review of the literature. *Urol Oncol* 2012;30:476-481
7. Nojima H, Cho A, Yamamoto H, Nagata M, Takiguchi N, Kainuma O, et al. Renal cell carcinoma with unusual metastasis to the gallbladder. *J Hepatobiliary Pancreat Surg* 2008;15:209-212
8. Backman H. Metastases of malignant melanoma in the gastrointestinal tract. *Geriatrics* 1969;24:112-120
9. Barretta ML, Catalano O, Setola SV, Granata V, Marone U, D'Errico Gallipoli A. Gallbladder metastasis: spectrum of imaging findings. *Abdom Imaging* 2011;36:729-734
10. Kim SY, Kim KW, Kim AY, Ha HK, Kim JS, Park SH, et al. Bloodborne metastatic tumors to the gastrointestinal tract: CT findings with clinicopathologic correlation. *AJR Am J Roentgenol* 2006;186:1618-1626
11. Yoshimitsu K, Honda H, Shinozaki K, Aibe H, Kuroiwa T, Irie H, et al. Helical CT of the local spread of carcinoma of the gallbladder: evaluation according to the TNM system in patients who underwent surgical resection. *AJR Am J Roentgenol* 2002;179:423-428
12. Kim SJ, Lee JM, Lee JY, Choi JY, Kim SH, Han JK, et al. Accuracy of preoperative T-staging of gallbladder carcinoma using MDCT. *AJR Am J Roentgenol* 2008;190:74-80
13. Horton KM, Fishman EK. Current role of CT in imaging of the stomach. *Radiographics* 2003;23:75-87
14. Scatarige JC, DiSantis DJ. CT of the stomach and duodenum. *Radiol Clin North Am* 1989;27:687-706
15. Jin KN, Lee JM, Kim SH, Shin KS, Lee JY, Han JK, et al. The diagnostic value of multiplanar reconstruction on MDCT colonography for the preoperative staging of colorectal cancer. *Eur Radiol* 2006;16:2284-2291
16. Lee JH, Lee JM, Kim SJ, Baek JH, Yun SH, Kim KW, et al. Enhancement patterns of hepatocellular carcinomas on multiphasicmultidetector row CT: comparison with pathological differentiation. *Br J Radiol* 2012;85:e573-e583
17. Lee JM, Choi BI. Hepatocellular nodules in liver cirrhosis: MR evaluation. *Abdom Imaging* 2011;36:282-289
18. Sun MR, Ngo L, Genega EM, Atkins MB, Finn ME, Rofsky NM, et al. Renal cell carcinoma: dynamic contrast-enhanced MR imaging for differentiation of tumor subtypes--correlation with pathologic findings. *Radiology* 2009;250:793-802
19. Levy AD, Murakata LA, Rohrmann CA Jr. Gallbladder carcinoma: radiologic-pathologic correlation. *Radiographics* 2001;21:295-314; questionnaire, 549-555
20. Lane J, Buck JL, Zeman RK. Primary carcinoma of the gallbladder: a pictorial essay. *Radiographics* 1989;9:209-228
21. Ishiguro S, Onaya H, Esaki M, Kosuge T, Hiraoka N, Mizuguchi Y, et al. Mucin-producing carcinoma of the gallbladder: evaluation by magnetic resonance cholangiopancreatography in three cases. *Korean J Radiol* 2012;13:637-642
22. Westacott SM, Mahraj R. *Anatomy and imaging of the normal gallbladder*. In: Meilstrup JW, ed. *Imaging atlas of the normal gallbladder and its variants*. Boca Raton: CRC Press, 1994:4
23. Edge SB, Byrd DR, Compton CC, Fritz AG, Greene FL, Trotti A, et al. *AJCC Cancer Staging Manual*, 7th ed. New York: Springer-Verlag, 2010:211-217
24. Jang JY, Kim SW, Lee SE, Hwang DW, Kim EJ, Lee JY, et al. Differential diagnostic and staging accuracies of high resolution ultrasonography, endoscopic ultrasonography, and multidetector computed tomography for gallbladder polypoid lesions and gallbladder cancer. *Ann Surg* 2009;250:943-949
25. Jung SE, Lee JM, Lee K, Rha SE, Choi BG, Kim EK, et al. Gallbladder wall thickening: MR imaging and pathologic correlation with emphasis on layered pattern. *Eur Radiol* 2005;15:694-701